Micro-vibration parameters fast demodulation algorithm and experiment of self-mixing interference*

WANG Xiu-lin (王秀琳)[1], **WANG Lu** (王路)[2], **CHEN Min-liang** (陈敏亮)[2], and **HUANG Wen-cai** (黄文财)[2]**

1. Department of Physics, Jimei University, Xiamen 361021, China

2. Department of Electronics Engineering, Xiamen University, Xiamen 361005, China

(Received 9 April 2014)

Self-mixing interference (SMI) technique can be used for measuring vibration, displacement, velocity and absolute distance. In this paper, a simple demodulation algorithm for fast measuring frequency and amplitude of a simple harmonic vibration target is proposed based on the basic theoretical model of self-mixing interference effects. The simulative results show that the error between the vibration parameters which are demodulated by this algorithm and initial settings merely results from the sample rate. Further, the experimental system of self-mixing vibration measurement is built. The experimental results have a good agreement with simulation analyses. The maximum error of frequency demodulation is less than 1 Hz in our experiment.

Document code: A **Article ID:** 1673-1905(2014)04-0304-4

DOI 10.1007/s11801-014-4059-x

Self-mixing interference (SMI) as a well-known and viable technique has attracted more and more attention. In the SMI measurement system, a laser beam is focused on an external object and then reflected or scattered back into the laser cavity, causing the modulation of lasing frequency and output power. The SMI signal which carries the information of the irradiated target is suitable for the measurement of vibrations, displacements, velocities and distances[1-5]. Compared with other traditional Michelson and Mach-Zehnder heterodyne interference measuring technologies, the main advantages of SMI technique are simplicity, compactness, robustness, low cost and no restriction by laser source[6,7]. In past decades, many researchers have analyzed the theory and observed the experimental phenomena of SMI in different types of laser. The displacement waveforms reconstruction in SMI has also aroused great concern[8,9].

In this paper, we present a simple demodulation algorithm for quickly measuring frequency and amplitude of a simple harmonic vibration target. The simulative result shows that the algorithm can quickly and efficiently modulate micro-vibration parameters of external object, and the error is quite small. Meanwhile, the experimental setup is built for the vibration measurement.

Nowadays, there are two general theoretical models for analyzing the SMI effect in semiconductor laser. One is strictly solving the Lang and Kobayashi rate equation[10], and the other is using a three-mirror cavity Fabry-Perot (FP) model[11] to analyze. The mathematical forms of SMI theoretical models on basis of the above two methods are the same, which can be written as

$$P(\phi) = P_0[1 + mF(\phi)] , \tag{1}$$

where P_0 is the laser power without optical feedback, and m is the modulation index. The laser phase ϕ is subject to the feedback given by the phase equation:

$$\phi = \phi_0 - C\sin[\phi + \arctan(\alpha)] , \tag{2}$$

where α is semiconductor laser line broadening factor, and C is optical feedback factor which represents the strength of the external optical feedback. ϕ_0 is the optical phase of the external path in the absence of feedback, given by $\phi_0=2kL=4\pi L/\lambda$ with k being the wave vector, λ being the wavelength and L being the variation of distance from the laser diode (LD) to the target. ϕ is the optical phase with feedback $F(\phi)$ is a periodic function whose shape depends on the feedback strength parameter C[12,13], which in turn depends on laser parameters, such as mismatch coefficient, target distance and laser cavity length. At present, the typical value of C is between 0.1 and 4.6 in most of SMI sensing applications. When the system stays in weak feedback regime, $F(\phi)$ is a cosine function, like expected in a normal interferometer.

For external harmonic (sine or cosine) vibrating object, the equation of the motion can be written as

$$L(t) = L_0 + \Delta L\sin(2\pi ft + \varphi) , \tag{3}$$

where L_0 is the initial distance between the outlet end of

* This work has been supported by the National Natural Science Foundation of China (No.61308048), the Natural Science Foundation of Fujian Province (No.2013J01244), and the Li Shangda Foundation in discipline construction (No.C513030).

** E-mail: huangwc@xmu.edu.cn

the laser and the external object, ΔL is the vibration amplitude of the object, f is the vibration frequency, φ is the initial phase, and t is the time variable. We set ΔL=1 μm, f=200 Hz and φ=5π/6. The vibration of the object is shown in Fig.1(a), and the simulated results of the SMI signal waveform with weak feedback (C=0.8) and moderate feedback (C=2.5) are shown in Fig.1(b) and (c), respectively. As can be seen from Fig.1(b), the SMI signal presents a sinusoidal waveform in the case of weak feedback level, which is similar to the conventional interference signal. In the case of C=2.5, i.e., in moderate feedback level, the self-mixing signal shows a sawtooth waveform. The top fringes move upward gradually, the below fringes move downward gradually, and the inclination of the signal also increases, as shown in Fig.1(c). When the displacement of reflecting objects is increased, the sawtooth waveform leans to the right, and when the displacement of reflecting objects is decreased, the sawtooth waveform leans to the left. At this time, the SMI signal is more suitable for practical measurement applications.

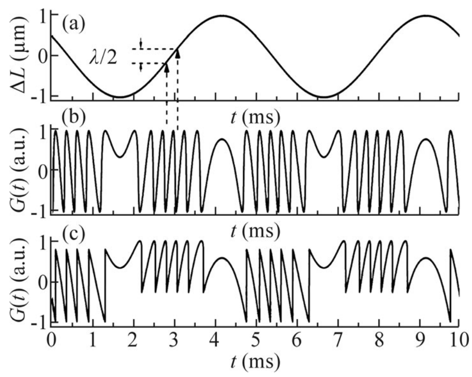

Fig.1 (a) The vibration of the object and simulated results of self-mixing signals for (b) *C*=0.8 and (c) *C*=2.5

Assuming that the SMI signal which is obtained in the experiment shown in Fig.2(a) is similar to the conventional interference, each interference fringe corresponds to $\lambda/2$ change of displacement. Then the vibration parameters of the object can be demodulated by differentiation and smoothing, as shown in Fig.2(b). After these processes, we can see from the SMI signal that when the displacement of external vibration object is increased, the pulse sequence signal is negative, while when the external object vibration displacement is reduced, the pulse sequence signal is positive. According to the position where positive and negative pulses of differential signal flip, the reverse segment of original SMI signal is identified. In each interval, SMI signal has an extremum point that can determine the reverse point, such as R_0, R_1 and R_2 in Fig.2(a), and the reverse point appears in the case that the vibration displacement reaches a maximum or minimum. According to the periodic vibration, any adjacent time interval between reverse points in SMI signal is a half cycle of object vibration. Assuming two corresponding adjacent time points of SMI signal reverse point are t_{R0} and t_{R1}, the frequency of vibration can be drawn as

$$\hat{f} = \frac{1}{2(t_{R1} - t_{R0})} . \tag{4}$$

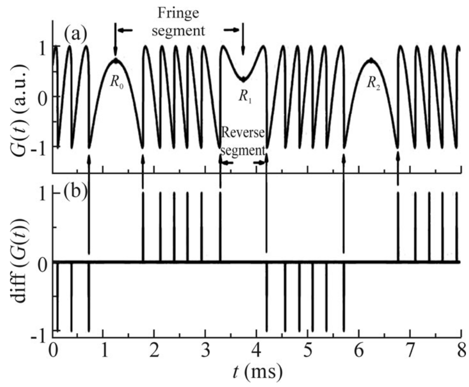

Fig.2 (a) SMI signal and (b) pulse train for extracting reverse points

Fig.3 shows the enlarged image of any two adjacent reverse points of the SMI signal which forms a fringe segment. As shown in Fig.3, the location of the signal minimum value from the fringe segment is found out and sequentially marked as 1 to j. There is a stripe between any two adjacent minimum values, which means that the displacement of object vibration is $\lambda/2$. Start measurement at t_{R0} from a reverse point R_0, and then the external vibration can be set as

$$y(t) = \pm \Delta L \cos[2\pi \hat{f}(t - t_{R0})] . \tag{5}$$

The displacement of object vibration is

$$|y(t_{i+1}) - y(t_i)| = \lambda / 2, \ i \in (1, j-1) . \tag{6}$$

Then the amplitude can be solved as

$$\Delta \hat{L} = \frac{1}{2(j-1)} \sum_{i=1}^{j-1} \left| \frac{\lambda}{\cos 2\pi f(t_{i+1} - t_{R0}) - \cos 2\pi f(t_i - t_{R0})} \right| . \tag{7}$$

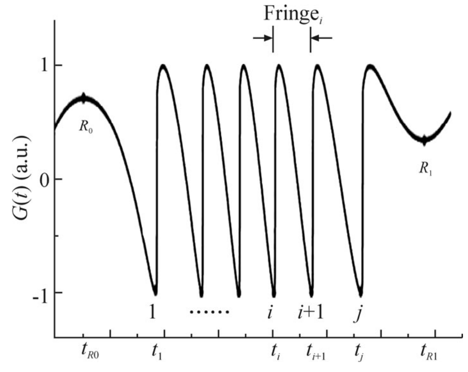

Fig.3 A fringe segment of SMI signal

Setting the same sampling interval (2 μs) and sampling points (2 500), the SMI signals at different feedback factors, frequencies and amplitudes of vibration are simulated. Then the parameters demodulated by this fast algorithm are shown in Tab.1. As shown in Tab.1, the algorithm is not affected by optical feedback factor. The demodulation of frequency and amplitude has high precision under different vibration parameters. The maximum errors of frequency and amplitude demodulation are 0.2 Hz and 0.004 μm, respectively. Besides, the algorithm can demodulate the signal as long as there is a complete stripe in stripe region since the measurement accuracy of typical self-mixing interference is $\lambda/2$. Further simulations show that the errors of demodulated vibration parameters are mainly affected by the sampling rate[14]. When the ratio of the sampling frequency to the vibration frequency is not integer multiple, it will lead to that the position of reverse point is not accurate. Moreover, when the amplitude is large, i.e., the number of stripes is too much between reverse points, the position of the SMI signal stripe obtained by initial simulation will also have some deviation. Therefore, through the demodulation algorithm at the same sampling rate, the error of the amplitude value will increase along with the increase of amplitude. In this case, by increasing the sampling rate, it will reduce the error effectively.

Tab.1 Simulation results and errors

C	f(Hz)	$\hat{f}$(Hz)	E_f(Hz)	ΔL(μm)	$\Delta\hat{L}$(μm)	$e_{\Delta L}$(μm)
				1	0.999 8	0.000 2
	240	240.16	0.16	3	2.999 5	0.000 5
				5	4.999 3	0.000 7
				1	1.000 3	0.000 3
0.7	370	369.82	0.18	3	3.002	0.002
				5	5.004	0.004
				1	1.000 5	0.000 5
	470	469.92	0.08	3	2.999	0.001
				5	5.001 2	0.001 2
				1	1.000 1	0.000 1
	240	240.16	0.16	3	3.000 3	0.000 3
				5	5.002 3	0.002 3
				1	0.999 4	0.000 6
2	370	369.82	0.18	3	3.003 3	0.003 3
				5	5.005 9	0.005 9
				1	0.999 9	0.000 1
	470	469.92	0.08	3	3.002 6	0.002 6
				5	5.004	0.004

The schematic diagram of experimental setup used to investigate the self-mixing vibration measurement is shown in Fig.4. An LD (FU650AD5_C9N) is used as the light source, which emit laser at 650 nm up to 5 mW on a single longitudinal mode and is fed by a constant current supply. The laser beam divergence is adjusted by the micro-lens which is packaged in the laser output. The laser emitted by LD irradiates onto the surface of vibrating speaker which is pasted by the reflective film. The optical power can be detected by a photodetector (PD) which is packaged in the tail of laser. Optical processing circuit is composed of transimpedance, amplifier and filter. Sampling resistor is 10 kΩ, and reverse magnification is 50. The second order Butterworth low-pass filter is used as the filter circuit. Its cutoff frequency is 10 kHz, and the quality factor is 0.707. The signal after filtering and amplifying is displayed and acquisited through the oscilloscope.

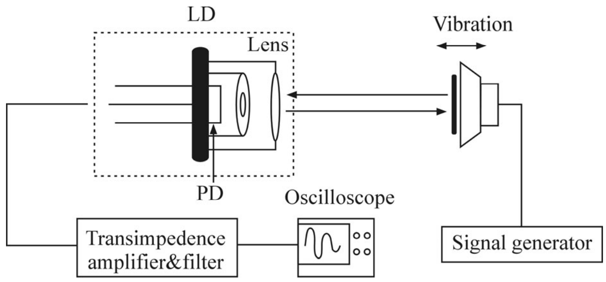

Fig.4 Experimental setup of vibration measurement in SMI

In our experiment, the distance between LD and speaker is about 12.5 cm. In order to get a better self-mixing signal, we adjust the micro-lens packaged on the section of laser output to focus the laser just landed on the vibration surface of the loudspeaker. Two groups of typical SMI signals are obtained by adjusting the function generator to make the amplitude and frequency of speaker change, as shown in Fig.5. Since noises inevitably exist in circle processing and optical feedback, it will lead to the error of feature point extraction during the signal demodulation. Therefore, we first use the filtering algorithm to smooth the experimental SMI signal. Then,

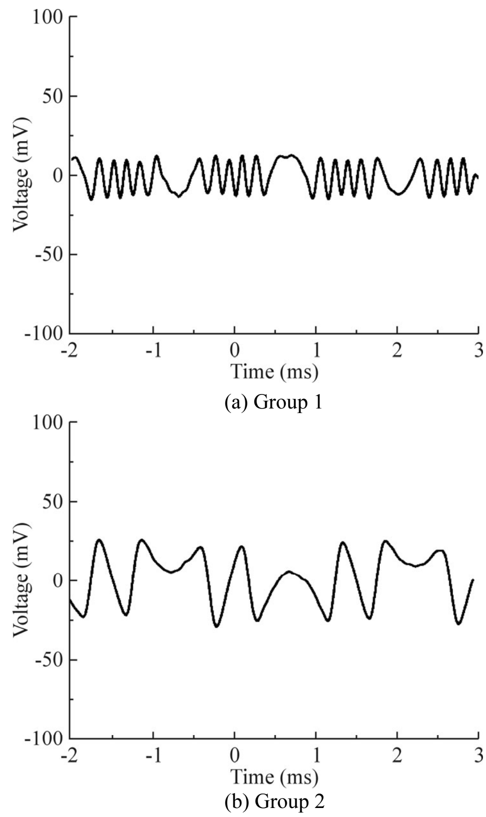

Fig.5 Typical SMI signals of vibration measurement

the frequency and amplitude of vibration are demodulated successfully by the demodulation algorithm mentioned above. The results are shown in Tab.2. The experimental frequency of speaker is given by the drive frequency of function generation. From Tab.2 we can see that the demodulation error of frequency is quite small compared with the actual value. When the drive frequencies are 370 Hz and 340 Hz, the corresponding demodulated frequencies are 369.55 Hz and 339.21 Hz, respectively. Frequency demodulation error is less than 1 Hz which is slightly larger than the simulation error. The amplitude value is also demodulated as shown in Tab.2. Since the actual amplitude value of speaker is unknown, the demodulation error of amplitude can not be given. As mentioned above, the demodulation errors of the frequency and amplitude depend on the sampling frequency. Although the error will be further amplified by the influence of noises in actual measurement, the demodulation result of amplitude still has a high credibility.

Tab.2 Experimental results and the errors

	f(Hz)	$\hat{f}$(Hz)	e_f(Hz)	$\Delta\hat{L}$(μm)
(a)	370	369.55	0.45	0.887 7
(b)	340	339.21	0.79	0.321 1

In conclusion, a fast demodulation algorithm which can measure the frequency and amplitude of simple harmonic vibration is proposed based on the basic theoretical model of laser SMI effect. The experimental setup of SMI micro-vibration measurement system is built for actual measurement and demodulation. The experimental results are in good agreement with the simulations. The maximal demodulation error of the frequency in experiment is less than 1 Hz. The demodulation algorithm can demodulate the frequency and amplitude quickly and correctly not affected by the strength of feedback. Therefore, it will have potential applications in the measurement of micro-vibration.

References

[1] K. Otsuka, K. Abe, J.-Y. Ko and T.-S. Lim, Optics Letters **27**, 1339 (2002).

[2] C. Bes, G. Plantier and T. Bosch, IEEE Transactions on Instrumentation and Measurement **55**, 1101 (2006).

[3] L. Scalise, Y. Yu, G. Giuliani, G. Plantier and T. Bosch, IEEE Transactions on Instrumentation and Measurement **53**, 223 (2004).

[4] F. Gouaux, N. Servagent and T. Bosch, Applied Optics **37**, 6684 (1998).

[5] YANG Ying, LI Xing-fei, KOU Ke and WANG Cuo, Journal of Optoelectronics·Laser **24**, 1075 (2013). (in Chinese)

[6] J. R. Tucker, A. D. Rakic, C. J. O'Brien and A. V. Zvyagin, Applied Optics **46**, 611 (2007).

[7] D. Han, M. Wang and J. Zhou, Optics Express **14**, 3312 (2006).

[8] Fan Y. L., Yu Y. G., Xi J. T. and Chicharo J. F., Applied Optics **50**, 5064 (2011).

[9] Zhang Yuyan, Zheng Mingyue and Du Xiaohong, Chinese Journal of Scientific Instrument **33**, 1351 (2012).

[10] R. Lang and K. Kobayashi, IEEE Journal of Quantum Electronics **16**, 347 (1980).

[11] W. M. Wang, K. T. V. Grattan, A. W. Palmer and W. J. O. Boyle, Journal of Lightwave Technology **12**, 1577 (1994).

[12] G. Giuliani, M. Norgia, S. Donati and T. Bosch, Journal of Optics A, Pure and Applied Optics **4**, 283 (2002).

[13] ZHANG Yu-yan, HU Wei, JIAN Xiong and XU Dan-qin, Journal of Optoelectronics·Laser **24**, 1150 (2013). (in Chinese)

[14] Xuguang Cai, Liang Lu, Jialiang Deng, Yang Huang, Shenglai Zhen and Benli Yu, Optik **124**, 932 (2013).